FABRICATION, CHARACTERIZATION AND PERFORMANCE OF GRAPHENE OXIDE-BASED FILTRATION DEVICES

FABRICACIÓN, CARACTERIZACIÓN Y COMPORTAMIENTO DE DISPOSITIVOS DE FILTRACIÓN BASADOS EN GRAFENO

A. A. Oliveira[a], J. A. G. Carrio[a,b†]

a) Mackenzie University, Sao Paulo, Brazil.
b) National University of Singapore, Singapore. juan.carrio@nus.edu.sg.†
† corresponding author

Recibido 18/10/2024; Aceptado 20/11/2024

Graphene oxide (GO) has been the subject of numerous studies due to the anomalous water transport through membranes of layered, laminated structures. The discovery of this phenomenon opened up the possibility of using GO in various applications related to nanofluids and nanofiltration and its potential integration in separation methods in industries. In the most accepted model, a few layers of water fill two-dimensional capillaries of an interconnected structure of GO sheets. Studies have shown that high pressures can induce slight chemical modifications in GO. Using high flow rates and thin membranes is economically preferable. In this work, filtration elements based on GO were fabricated under high pressure to primarily achieve these conditions. A nanostructured device was obtained, capable of filtering for over 29 hours with stability and efficacy in different aqueous solutions of organic dyes and clay particle suspensions up to the detection limit of UV-Vis spectroscopy. Additionally, it exhibited a rejection rate of 90 % to 100 % for trivalent and divalent cations in saline solutions. A comparative study on GO treated directly with a metal and a polymeric material under high pressures is presented. The presence of the metal at high pressures led to a partial reduction of the GO, which caused significant surface modification. Conversely, the presence of the polymer helped preserve functional groups both on the surface and in the inner layers of the devices, which resulted in a structure that allowed for a constant flow of saline solutions containing organic and inorganic contaminants.

El óxido de grafeno (GO) ha sido objeto de numerosos estudios debido al transporte anómalo de agua a través de membranas de estructuras laminadas en forma de capas. El descubrimiento de este fenómeno abrió la posibilidad de utilizar GO en diversas aplicaciones de nano-fluidos y nanofiltración, así como su potencial integración en métodos industriales de separación. En el modelo más aceptado, unas pocas capas de agua llenan capilares bidimensionales de una estructura interconectada de hojas de GO. Estudios han demostrado que altas presiones pueden inducir ligeras modificaciones químicas en el GO. Usar altas tasas de flujo y membranas delgadas es económicamente preferible. En este trabajo, se fabricaron filtros de GO usando alta presión para ese fin. Los dispositivos nano-estructurado, filtraron durante más de 29 horas con estabilidad y eficacia soluciones acuosas de colorantes orgánicos y suspensiones de partículas de arcilla hasta el límite de detección de la espectroscopía UV-Vis. La tasa de rechazo alcanzó del 90 % al 100 % para cationes trivalentes y divalentes en soluciones salinas. Este estudio compara el GO tratado a altas presiones en contacto directo con un metal y con un material polimérico. La presencia del metal condujo a una reducción parcial del GO, lo que causó una modificación significativa de la superficie. Por el contrario, la presencia del polímero ayudó a preservar los grupos funcionales tanto en la superficie como en las capas internas de los dispositivos, lo que resultó en una estructura que permitió un flujo constante de soluciones salinas conteniendo contaminantes orgánicos e inorgánicos.

PACS: Graphene oxide (óxido de grafeno); water filtration (filtración de agua); nanofluids (nanofluidos).

I. INTRODUCTION

The concerns about environmental conditions are reaching various social, political, and economic segments as the problem affects humanity. There is a global discussion about environmental management, nature preservation, water scarcity, and efforts to educate people about environmental conservation. Meanwhile, the availability of fresh and drinkable water on the planet continues to decrease. Brazil holds around 16 % of the planet's total freshwater reserves and has the largest river and underground aquifer. The country still has a higher water availability per cubic meter per person than most countries worldwide. Even so, water filtration and purification from wastewater are necessary in many regions across the country [1, 2].

There is intense research on new processes and materials for water purification and desalination due to the drawbacks of today's commercial methods of Reverse Osmosis (RO) and thermal desalination, mainly related to their large energy footprints. Graphene and its variants have become one of the materials with the most significant potential for the fabrication of membranes with salt rejection of around 99 % and water permeability of around 100 L/cm^2.day.MPa, which is two orders higher than commercial RO membranes. Devices based on GO are strong candidates for water desalination and wastewater purification applications due to their selective properties of water over other molecules [3, 4]. On the other side, graphite, the natural precursor of the graphene materials family, is among the many abundant minerals available in Brazil and is widely used in the Brazilian industry [5, 6].

Nanostructured GO membranes are composed of layers of oxidised graphene sheets stacked on each other, with

oxygen-containing functional groups separating them. A frictionless water flow is attributed to pristine graphene regions forming nanochannels due to the non-uniform distribution of the chemical groups [3]. These laminates have excellent properties that make them suitable for use in membranes, including water dispersibility, hydrophilicity, a negatively charged surface, and scalability in production. As a result, GO-based membranes have been extensively researched for potential applications in water purification, organic solvent filtration, gas separation, and desalination through membrane distillation, among other uses [7, 8].

The fabrication process of laminate membranes still presents several challenges, especially at scales larger than the laboratory level. Today's most common method at research laboratories is still vacuum filtration [9–11]. However, variables such as vacuum pressure, filtration volume, solid-liquid ratio, and other method-specific parameters can significantly impact the outcomes. This variability makes it difficult to compare different batches of membranes and various studies, leading to inconsistent results. This work uses a different approach to fabricating GO filtration devices: common compaction by uniaxial pressure has been applied to conform GO powder into mechanically stable membranes. This treatment leads to a microstructure different from the ordered laminates widely described in the literature.

II. EXPERIMENTAL

II.1. Synthesis of graphene oxide

A modified Hummers method was used to synthesise graphene oxide 12 13. Briefly, graphite powder obtained from industrial waste was set to oxidise by stirring in a mixture of concentrated sulfuric acid and phosphoric acid in the proportion 98 %/2 % w/w. Immediately, the mixture was kept at 0 °C to prevent rapid heat generation, and potassium permanganate was added under vigorous stirring for 0.5 hours. The reaction mixture was heated to 40 °C for 4 hours and then stirred at room temperature for 8 hours. Hydrogen peroxide and ice were added to remove the remaining unreacted potassium permanganate and manganese dioxide. The purification process of GO was performed by several cycles of centrifugation and dispersion in deionised water. Finally, ultrasonication was applied for exfoliation. The suspension was stable, and its Zeta potential of approximately -40 mV was measured using a Zetasizer Nano ZS device.

II.2. Sample characterisation

The UV-visible spectroscopy (UV-Vis) characterisation of the liquids was performed using an Agilent 8453 spectrophotometer. Fourier Transform Infrared Spectroscopy (FTIR) spectra of the samples were taken with a Spectrum BX spectrophotometer from Perkin Elmer. The GO chemical composition was determined by CHNS Elemental Analysis. A low-energy Scanning Electron Microscopy (SEM) (5 kV) from HITACHI, model H3000, was employed to perform surface analysis of non-conductive materials, and a high-energy SEM from JEOL, model JSM6510, was used for samples covered with conductive carbon layer. GO samples were also analysed using a Witec Alpha R300 confocal Raman microscope with a 532 nm laser line and a power of 5 mW, and the thickness measurements were performed in an AFM Bruker Dimension Icon. A milliohmeter Agilent HP 4338B was used to measure electrical resistance measurements of the compacted samples by the four-point probe or Kelvin method. X-ray powder diffraction (XRD) data were collected with a conventional Bragg-Brentano geometry diffractometer, model Rigaku MiniFlex II, using CuKα radiation, with a fixed monochromator and slits. The experimental conditions in step-scan mode were: 30 kV, 15 mA, $3^\circ \leq 2\theta \leq 120^\circ$, step $2\theta = 0.01^\circ$, and a counting time of 1 second.

III. RESULTS AND DISCUSSION

The applied process was designed to minimise costs as much as possible, so it was considered that the resulting product, although still containing impurities or not fully exfoliated, could be used for specific applications, such as industrial water filtration. Fig. 1 shows the final brown powder and some steps of the oxidation and exfoliation process applied to low-cost graphite.

III.1. Fabrication of filtration devices

Compressed pellets in the form of discs were made using 5 g of GO dry powder. The powder was subjected to a uniaxial pressure of 12 MPa for 20 minutes using stainless steel matrixes of 3.0 cm and 1.5 cm diameter at room temperature.

From ten samples, five were pressed in direct contact with the metallic matrix (hereafter named GOM), and five were encapsulated on the top and bottom by Teflon discs with the same diameter (hereafter named GON). The final shape of all samples is a disc with average dimensions of 3 cm and 1.5 cm in diameter and 3 mm in height.

Figure 2 shows two of the obtained discs; one pressed with direct contact with the stainless-steel matrix (GOM) (a) and the other pressed between two polymeric discs (GON) (b), one of which is the white disc shown on the top of the GO.

III.2. Electrical resistivity measurement

The electrical resistance was measured using a four-point probe in each compacted sample. Twenty values were collected for each sample, and the measurements were repeated on four different days, considering the high sensitivity of GO to the environment humidity. The equipment collects 32 values for each resistance measurement. The average electrical resistance of the GON discs was R_{GON} = (2681 ± 159) Ω, while the average for the GOM samples was R_{GOM} = (1373 ± 112) Ω, almost half of the electrical resistance of the samples pressed with the polymer. The main source of uncertainty is the fluctuations in environmental humidity,

so the standard deviations can be regarded as a measure of uncertainty. Since the electrical conductivity of GO can only increase if the functional groups decrease, this result indicates that direct contact with metal under high pressure causes a partial reduction process, leading to an increase in conductivity, at least on the sample surface. This result also agrees with descriptions in the literature, where GO can be considered both an insulator and a semiconductor, depending on its preparation and modifications [14].

Figure 1. From left to right, stirring graphite in acid solution, hydrogen peroxide adding, and the final brown GO powder.

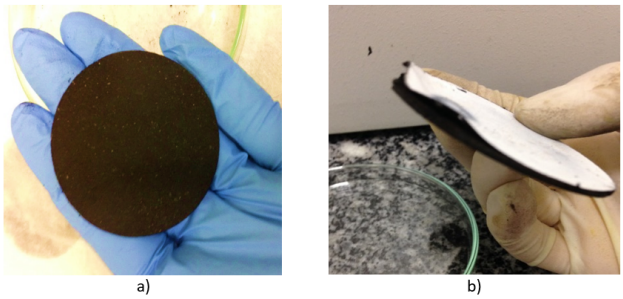

a) b)

Figure 2. GO compacted discs a) pressed directly in the metallic matrix and b) encapsulated in Teflon.

III.3. Characterisation by Scanning Electron Microscopy (SEM)

The SEM images in Fig. 3 clearly show the difference between the surfaces of the samples. Fig. 3a) corresponds to the GOM sample, which is apparently well compact and has a smooth graphene-like surface. In contrast, Fig. 3b) shows the irregular surface of the GON sample, in which, despite being subjected to the same fabrication conditions, the GO sheets are not so well compacted. This leads us to hypothesise that the functional groups are preserved due to the presence of the polymer. Additionally, there is an increase in physical cross-linking caused by the interaction of GO functional groups under high pressure. As a result, the preservation of the functional groups leads to a rough, less graphene-like surface.

The semiquantitative EDS analysis of the precursor GO showed a mass proportion of carbon and oxygen of 57.69 % and 35.36 %, respectively.

III.4. CHNS Elemental Analysis

The synthesised GO contains 53.85 % carbon, 3.27 % hydrogen, 1.40 % nitrogen, 1.14 % sulfur, and 40.34 % oxygen. This result is compatible with the oxygen content detected by semiquantitative EDS.

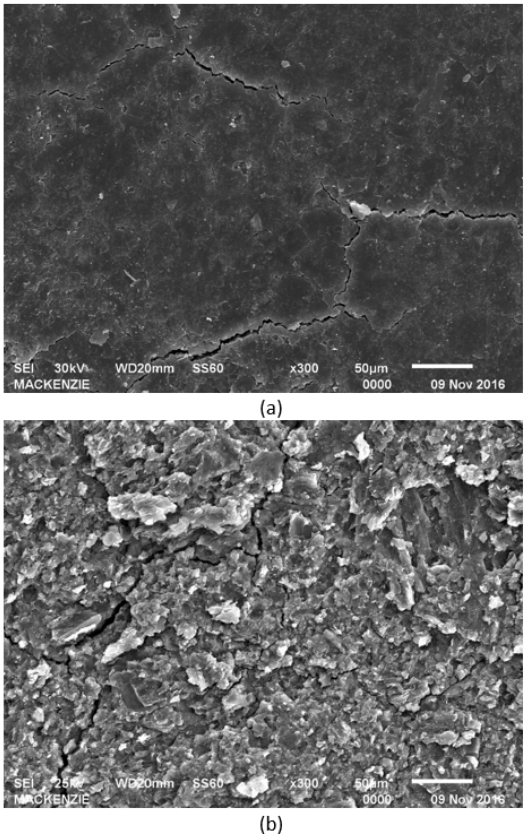

Figure 3. SEM images of the surfaces of a GOM sample in a) and a GON sample in b).

III.5. X rays powder diffraction analysis (XRD)

A comparison of the X-ray diffractograms of the compacted samples shows a difference in the position of the peak of the (002) planes, as shown in Fig. 4. The diffraction peak was fitted using a Pearson VII function, and the interplanar distance was determined by the Bragg equation. The sample encapsulated in polymer (GON) displays a distance between the layers that is clearly greater than that of the sample compacted in direct contact with the metallic matrix (GOM). Given that the diffractograms were collected under equal experimental conditions, this result may have two reasons: the polymer allows the functional groups of the GO to remain intact or contributes to the preservation of the presence of water between the GO layers, leading to a greater interplanar distance. Since the compaction process is conducted in just 20 minutes, it can be considered that this is not a sufficient period for water loss that could cause this effect. Therefore, we can conclude that in the case of the metallic matrix, the metal must reduce the functional groups. Additionally, the diffractograms show the presence of non-exfoliated material.

This characterisation by XRD is superficial in relation to the thickness of the compacted samples, given that the penetration depth of the X-rays is on the order of dozens of layers of GO. The full width at half maximum (FWHM)

of the peaks is similar for both samples, indicating that there is no different effect of the processes on the crystallinity of the samples. Thus, the greater distance between the layers of the polymer-encapsulated sample, at least in the region close to the surface, promotes the rapid entry of water to the internal layers without dismantling the device during the filtration process. Structurally, the polymer-encapsulated sample allows water entry due to the greater interplanar distance. Chemically, the penetration of water should dissolve the GO in this sample, but this does not occur due to the cross-linking between the functional groups of the inner layers within the volume of the sample.

III.6. Fourier Transform Infrared Spectroscopy (FTIR)

Fig. 5a) presents the FTIR spectra of the compacted samples and the precursor GO. In the spectra of Fig. 5a), a high-intensity band appears at 3364.20 cm^{-1}, associated with the stretching mode between -OH and C-OH, caused by the presence of alcohol or water groups in the GO. The bands in the 1735 cm^{-1} region correspond to the stretching vibration bands of C=O in -COOH. The 1611 cm^{-1} bands are identified as the elongation of C=C unsaturation. A band at approximately 1400 cm^{-1} characterises the hydroxyl (-OH) on the surface of the graphene oxide structure. A band at approximately 1230 cm^{-1} characterises the bending modes in the C-O-C groups of the epoxy group. A band slightly above 1037 cm^{-1} characterises C-C, and a band just below 868.34 cm^{-1} corresponds to a C-O bond. These bands indicate that the oxidation of graphite occurred with the introduction of functional groups.

The modifications in the GO structure caused by the fabrication method of the filtration devices are visible through changes in the FTIR spectrum, as can be observed in Figures 5b) and 5c), which show the characteristics of the spectrum of the samples GOM and GON, respectively. In the GOM sample, there was a decrease in the high-intensity band at 3364.20 cm^{-1}, caused by the reduction of the water groups in the GO, resulting in a partial reduction of the GO. Additionally, we can observe an increase in various other bands, influencing the increase in physical cross-linking and resulting in higher resistance of the device when in contact with water.

III.7. AFM characterisation

The AFM characterisation allowed a description of the average morphology of the flakes, which exhibit wrinkles and curling, as illustrated in Fig 6. Consequently, determining the thickness of the material and estimating the number of layers of GO can only be done approximately. It is known that there is a space between the two-dimensional material and the substrate, often filled with water and air. Based on the profiles shown in Figure AFM, corresponding to the flakes in the same figure, it can be concluded that, on average, the analysed sample contains between 15 and 20 layers and has lateral dimensions of approximately 6 μm.

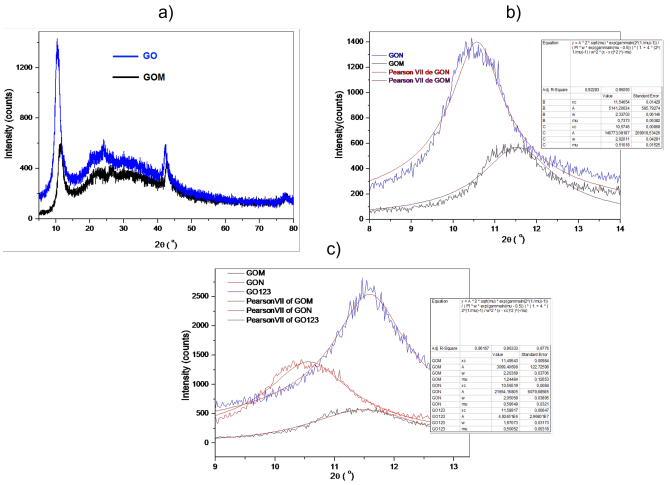

Figure 4. a) Diffractograms of the original GO powder (blue) and the sample fabricated in direct contact with the metallic matrix (black), b) Fitting of the diffraction peak corresponding to the (002) reflection of GO in the samples GON and GOM, and c) Comparison of the (002) reflection peaks of the original GO, GON and GOM.

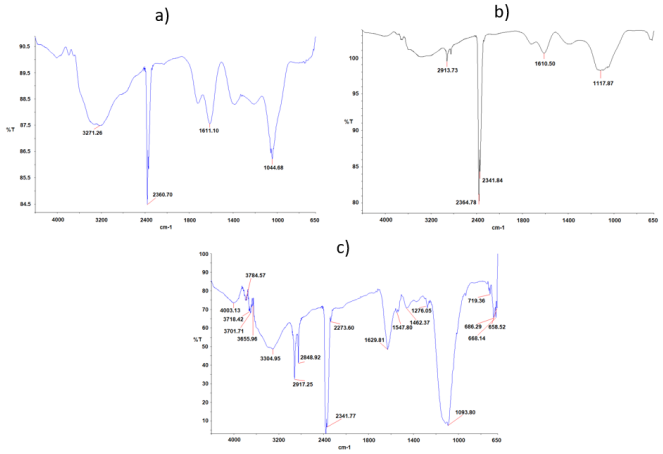

Figure 5. FTIR spectra of the a) precursor GO and the compacted samples, b) GOM, and c) GON.

III.8. Characterisation by Raman Spectroscopy

The Raman spectrum of GO consists of a broad band at approximately 1350 cm^{-1}, called the D band, which is commonly associated with defects in the graphitic structure related to sp^2 hybridisation (Fig. 7). The second band, known as the G band, is found near to 1600 cm^{-1}, corresponding in the graphitic structure to the first-order scattering of the tangential stretching mode (E_{2g}). The 2D band around 2680 cm^{-1} is attributed to second-order processes, where double resonance transitions produce two phonons with opposite momentum. Unlike the D band, which is Raman active only in the presence of defects, the 2D peak is active even in the absence of defects. A defect-activated peak called D+G is also visible around 2950 cm^{-1}. The edge of GO generally has more defects than its basal plane due to a higher amount of sp^3 hybridisations. Its spectrum also shows a shift in the G band, corresponding to a disorder of the sp^2 bonds. The D band shows almost no shift, but there is an increase in

the full width at half maximum, suggesting the formation of functional groups due to extensive oxidation.

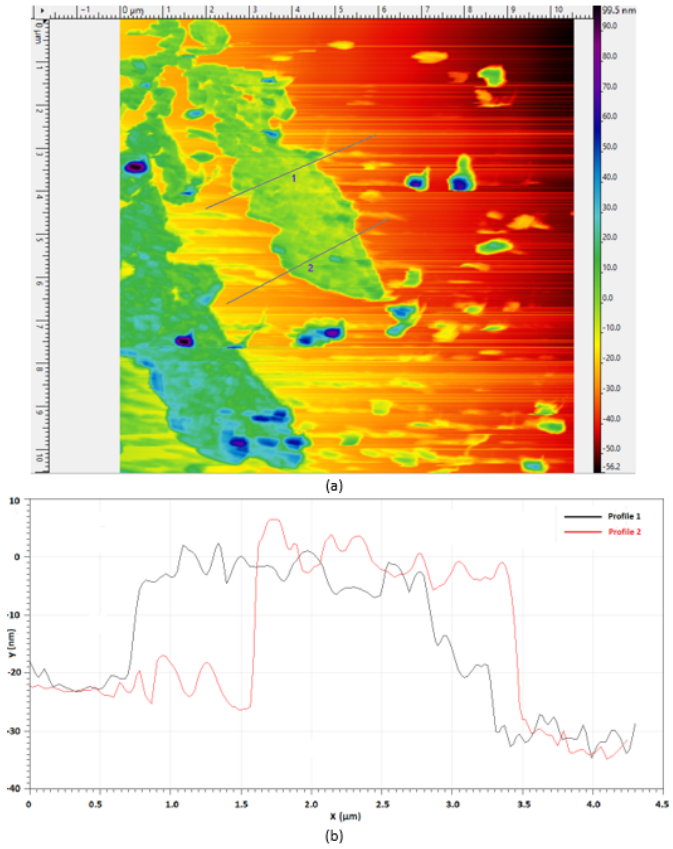

Figure 6. a) Average morphology and dimensions of GO flakes by AFM, and b) profile measurement of flake thickness.

The Raman spectra of three GON and three GOM samples, shown in Fig. 7, were analyzed using the metric proposed by [15], applying the Lorentz function for peak simulation. The peak at approximately 1,690 cm^{-1} is now called G_{app} and interpreted as composed of two modes, G and D'_{inf} (D' inferred). The difference in their positions, D'_{inf} - G_{app}, is related to the mass ratio of carbon to oxygen content (C/O), which varies among graphene oxide (GO), reduced graphene oxide (rGO), and graphene. Expressions (1) to (3) provide the criteria for classification.

Graphene Oxide (GO):

$$D'_{inf} - G_{app} < 0; \qquad C/O < 10 \tag{1}$$

Reduce graphene oxide (rGO):

$$0 < D'_{inf} - D_{app} < 25; \qquad 10 < C/O < 500 \tag{2}$$

Graphene:

$$D'_{inf} - G_{app} > 25; \qquad C/O > 500 \tag{3}$$

Table 1. Results from Raman spectra analysis

Sample	G_{app} position	D'_{inf} intensity
GON	1589.65	936
936GOM	1593.47	902

Furthermore, when GO is submitted to reduction, the position of the peak Gapp shifts to higher values, and the intensity of D' decreases. Our results for the energy differences between the G_{app} and D'_{inf} peaks indicate a low oxygen content in both cases. However, the positions of G_{app} and intensities of D'_{inf} indicate a partial reduction of GOM when compared to GON. The average results for each type, as shown in Table **??**, align with the tendency described in [15] when GO is reduced, and are consistent with our findings from SEM, FTIR, and UV-Vis.

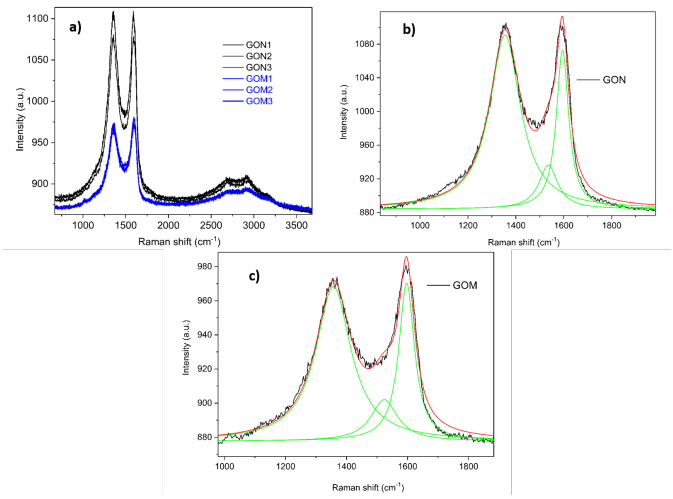

Figure 7. Raman spectra of a) 6 samples and two-peak fittings applied to the apparent peak G of b) GON and c) GOM.

III.9. Filtering experiments

The filtration experiments were carried out in a Büchner funnel without applying vacuum pressure. Samples of water containing organic dyes and clay particles, as well as others with a saline solution, were used to test the filtering discs. The GOM samples became mechanically unstable after a few minutes of contact with water, so they could not be used for water filtering. In contrast, all the GON discs were capable of continuing to filter the water solutions for at least 29 hours. The solutions filtered with the GON samples were characterised by UV-visible Spectroscopy (UV-Vis) and Inductively Coupled Plasma Emission Optical Spectroscopy (ICP-EOS).

Figure 8 presents the UV-Vis spectra of samples of the filtered solutions and a GO suspension in pure water for comparison. The UV-Vis spectrum of GO is shown in Fig. 8a. It exhibits a peak at around 233 nm, which is attributed to the $\pi - \pi*$ transitions in the C=C bonds, and a shoulder near 290 to 300 nm, arising from the $n - \pi*$ transitions in the C=O bonds [15,16]. Figure 8b shows the spectrum of the aqueous suspensions of clay particles and GO before and after filtration. The filtered sample shows a drop of approximately 50 % in absorbance. The experiment involved filtering 0.3 L of a solution at atmospheric pressure containing 5.1 g/L of clay

particles and 8.3 g/L of GO for 29 hours, resulting in a flow rate of 56.2 L/m^2.h.

Figure 8c presents the spectra of the experiment with a saline solution before and after filtration. Two filtration processes were carried out at atmospheric pressure. Initially, 0.3 L of the aqueous solution was filtered, followed by another 0.3 L of the same solution. The solution was prepared with known concentrations of salts and a suspension of 8.3 g/L of GO. This experiment lasted approximately 21 hours and resulted in a total flow rate of 129.5 L/m^2.h. One important observation from this experiment is that as the device undergoes the filtration process, the flow of the solution during the first 10 to 15 minutes is low and gradually increases until a certain constant value, and the resulting liquids show a greater reduction in absorbance. To accelerate the process, an experiment was performed by applying a vacuum pressure of around 0.5 bar. This was only necessary for the first 5 minutes to stabilise the flux. The pressure treatment can increase the cross-linking between the GO flakes, which can explain the enhancement of the bulk mechanical strength.

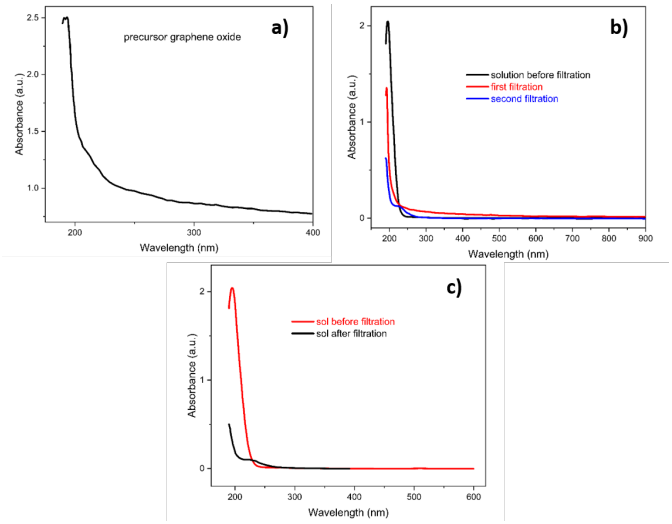

Figure 8. UV-Vis spectra of a) precursor GO suspension, b) and c) liquids before and after filtering experiments.

For salt filtration, solutions containing barium, chromium, sodium, and copper salts were used, all at a concentration of 100 ppm. An analysis using Inductively Coupled Plasma Emission Optical Spectroscopy (ICP-EOS) conducted to detect metal cations found that the filtering process resulted in the retention of Ba^{+2} at approximately 90 %, Cr^{+3} at around 98 %, Na+ at about 12 %, and Cu^{+2} at approximately 90 %.

IV. CONCLUSIONS

Using graphene oxide synthesised from low-cost graphite, nanostructured filtration devices were fabricated by a common compaction procedure of uniaxial pressure at room temperature. Graphene oxide pressed in direct contact with the metallic matrix suffered a partial reduction, which increased its electrical conductivity, caused a significant surface modification, and made it unstable in the presence of water. Conversely, the compaction of GO powders previously encapsulated in a polymer resulted in nanostructured filters with high mechanical strength. The devices could filter for over 29 hours with a flow rate of 56.15 L/m^2.h different aqueous solutions of organic dyes and clay particle suspensions up to the detection limit of UV-Vis spectroscopy. Additionally, although not specifically designed for this purpose, they exhibited a rejection rate of Ba^{2+} at around 90 %, Cr^{3+} at around 98 %, Na^{+} at around 12 %, and Cu^{+2} at around 90 %, highlighting that these results were obtained using a precursor that is cheaper than others available on the market. We concluded that the presence of the polymer helped preserve the functional groups on the surface of the devices and, together with the bulk effect of high pressure, the procedure resulted in a crosslinked structure that allowed a constant flow of aqueous saline solutions containing organic and inorganic contaminants. Further investigation is necessary to understand the observed effects of the high pressure, both on the superficial and bulk microstructure of GO, under different conditions.

REFERENCIAS

[1] BRASIL. Portaria n. 2914, de 12 de Dezembro de 2011, Diário Oficial Da União, Brasília, 12 Dez., (2011).

[2] Agência Nacional de Água – Disponibilizada à Rede Das Águas, Revista Agua Online, Manual Do Rio Tietê, Instituto Vidagua, (2016).

[3] S. Hong, C. Constans, M. V. Surmani Martins, Y. C. Seow, J. A. Guevara Carrió, S. Garaj, Nano Lett. **17**, 728 (2017).

[4] R. R. Nair, H. A. Wu, P. N. Jayaram, I. V. Grigorieva, A. K. Geim, Science **335**, 442 (2012).

[5] LIMA, D. B. de., Tese de Doutorado - Curso de Engenharia Elétrica, Escola Politécnica Da Universidade de São Paulo, (2011).

[6] NASCIMENTO, Jefferson J. P.- Tese de Doutorado - Curso de Engenharia, Centro de Desenvolvimento Da Tecnologia Nuclear, Comissão Nacional de Energia Nuclear, Belo Horizonte (2013).

[7] J. A. G. Carrio, Talluri, S. T. Toolahalli, S. G. Echeverrigaray, A. H. C. Neto, Sci. Rep. **13**, 9781 (2023).

[8] D. Cohen-Tanugi, J. C. Grossman, Nano Lett. **12**, 7 (2012).

[9] A. Pedico, L. Baudino, A. Aixalà-Perelló, Lamberti Membranes **13**, 429 (2023).

[10] C. H. Tsou et al., J. Membr. Sci. **477**, 93 (2015).

[11] J. A. G. Carrio, S. G. Echeverrigaray, V. P. Talluri, D. P. Sudhakaran, H. T. Gan, D. Gardenö, K. Friess, A. H. C. Neto, Int. J. of Hydrogen Energy **90**, 646 (2024).

[12] D. Bouša et al., Chem. Eur. J. **23**, 11416 (2017).

[13] D. C. Marcano et al. ACS Nano **4**, 4806 (2010).

[14] X. Huang, et al., Nanotechnology **23**, 455705 (2012).

[15] Q. Lai, S. Zhu, X. Luo, M. Zou, S. Huang, AIP Adv. **2**, 032146 (2012).

[16] T. Zhang et al. Microchim. Acta **186**, 207 (2019).